Allergy EUROPEAN JOURNAL OF ALLERGY AND CLINICAL IMMUNOLOGY

Allergy

ORIGINAL ARTICLE EXPERIMENTAL ALLERGY AND IMMUNOLOGY

Distant lymph nodes serve as pools of Th1 cells induced by neonatal BCG vaccination for the prevention of asthma in mice

G. Zhang[1,*], P. Wang[1,*], Z. Qiu[1], X. Qin[2], X. Lin[1], N. Li[1], H. Huang[1], H. Liu[1], W. Hua[1], Z. Chen[1], H. Zhao[3], W. Li[1] & H. Shen[1,4]

[1]Department of Respiratory and Critical Care Medicine, Second Affiliated Hospital, Zhejiang University School of Medicine, Hangzhou; [2]Department of Respiratory Disease, People's Hospital of Guangxi Zhuang Autonomous Region, Nanning, China; [3]Pulmonary & Critical Care Unit, Massachusetts General Hospital, Harvard Medical School, Boston, MA, USA; [4]State Key Lab of Respiratory Disease, Guangzhou, China

To cite this article: Zhang G, Wang P, Qiu Z, Qin X, Lin X, Li N, Huang H, Liu H, Hua W, Chen Z, Zhao H, Li W, Shen H. Distant lymph nodes serve as pools of Th1 cells induced by neonatal BCG vaccination for the prevention of asthma in mice. *Allergy* 2013; DOI: 10.1111/all.12099.

Keywords
asthma; Bacillus Calmette–Guérin; migration; neonatal vaccination; Th1 cells.

Correspondence
Dr Hua-Hao Shen, Department of Respiratory and Critical Care Medicine, Second Affiliated Hospital, Zhejiang University School of Medicine, Hangzhou 310009, China.
Tel.: (86) 571 87783729
Fax: (86) 571 87783729
E-mail: hh_shen@yahoo.com.cn

*These two authors contributed equally to this work.

Accepted for publication 26 November 2012

DOI:10.1111/all.12099

Edited by: Angela Haczku

Abstract

Background: Neonatal Bacillus Calmette–Guérin (BCG) vaccination induces vigorous T-helper type 1 (Th1) responses and inhibits allergy-related airway dysfunction, but the exact mechanisms remain unclear. The objective of this study was to address where the Th1 cells induced by neonatal BCG vaccination are generated and stored, and how they are recruited into the inflamed airway for the prevention of allergen-induced airway inflammation.

Methods: We vaccinated neonatal C57BL/6 mice with BCG in a mouse model of asthma and analyzed the expression and function of Th1 cells *in vivo* and *in vitro*.

Results: BCG vaccination–induced Th1 cells in the local inguinal lymph nodes (ILN) migrated into the lungs upon inhaled ovalbumin (OVA) challenge in OVA-sensitized mice. These $CD4^+$ T cells in the ILN exhibited potentials of activation, proliferation and cytokine secretion and expressed high levels of CXCR3. Adoptive transfer of $CD4^+$ T cells from BCG-treated ILN significantly decreased allergic airway responses. In addition, the protective effect of BCG vaccination against allergic airway inflammation was lost upon the excision of the ILN.

Conclusions: These data demonstrate that ILN serves as a 'weapon' pool of Th1 cells following BCG vaccination, and these cells are ready for the migration into the inflamed lungs upon the allergen challenge, thereby inhibiting allergen-induced airway disorder.

Allergic asthma is an immunodysregulatory disease that is mediated by excessive T-helper type 2 (Th2) immune responses to allergens in the lung (1–4). In contrast, antigen-induced Th1 responses and associated IFN-γ production can down-regulate Th2 responses, thereby inhibiting allergen-induced airway inflammation (5, 6).

Vaccination with Bacillus Calmette-Guérin (BCG) induces strong Th1 responses and Th1 cells infiltrating into the lung and then modulates the development of asthma in both rodents and humans (7–14). The accumulation of IFN-γ-expressing T cells may result from the migration of activated T cells from circulation and/or the rapid expansion of residual memory T cells in the lung (15, 16). Notably, BCG vaccination or chronic infection of mycobacterium tuberculosis (*M. tb*) usually fails to establish an effective memory T-cell immunity due to the long-term presence of sustainable antigen (17, 18). Furthermore, effector T cells can migrate into nonlymph target tissues

Abbreviations
BCG, Bacillus Calmette–Guérin; ILN, Inguinal lymph nodes; OVA, Ovalbumin; CFSE, 5-(and-6)-carboxyfluorescein diacetate, succinimidyl ester; MLN, Mediastinal lymph nodes.

© 2013 John Wiley & Sons A/S. Published by Blackwell Publishing Ltd

during the process of inflammation (19, 20). Therefore, it is likely that BCG-induced Th1 cells behave like these aforementioned effector T cells. However, where the IFN-γ-expressing Th1 cells induced by BCG vaccination are generated and stored and how these cells are recruited into the inflamed airway following OVA challenge have not been clarified.

In this study, we tested the hypothesis that some nickels might exist in the body where the enriched BCG-specific Th1 cells were stored and ready for migration into the inflamed lung to protect against allergic airway inflammation. We found inguinal lymph nodes (ILN), not the spleen or mediastinal lymph nodes (MLN), served as a pool of Th1 cells that were then recruited into the lung and ameliorated OVA-induced airway inflammation.

Materials and methods

Mice

C57BL/6 mice were from the Experimental Animal Center of Zhejiang University and housed in a specific pathogen-free facility. Both male and female neonates were used, and the experimental protocols were approved by the Ethical Committee for Animal Studies at Zhejiang University, China.

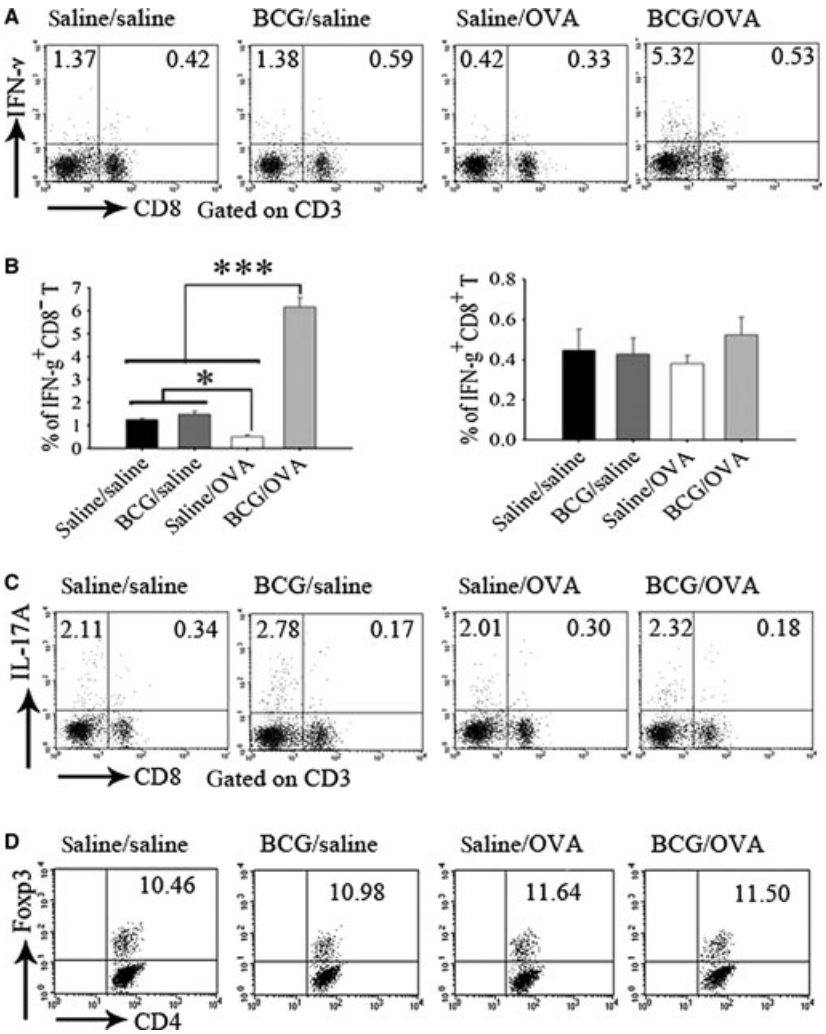

Figure 1 An increased frequency of Th1 cells in the lung of BCG-vaccinated mice upon OVA challenge. Groups of neonates were injected with saline or BCG and sensitized/challenged with saline or OVA later (termed saline/saline, saline/OVA, BCG/saline, and BCG/OVA). Forty-eight hours after the last OVA challenge, their lung tissues were dissected out for further analysis. (A–C) Representative FCM plots (A), quantitative analysis (B) of $CD3^+IFN\text{-}\gamma^+$ T cells, and representative FCM plots of $CD3^+IL17^+$ T cells (C) in the lung. Lymphocytes were isolated from the lungs of different groups of mice and stimulated with PMA/ionomycin *in vitro* for 5 h. The cells were then stained with PE-Cy5-CD3, FITC-CD8, and PE-IFN-γ or PE-IL-17A and gated on CD3 for FACS analysis. $CD3^+CD8^-$ T cells were considered as $CD4^+$ T cells in this experiment. (D) Representative FCM plots of $Foxp3^+CD4^+$ T cells in the lung. Data are expressed as the mean ± SEM of individual groups (n = 6–8 mice per group) from two separate experiments. *****$P < 0.05$; *******$P < 0.001$.

© 2013 John Wiley & Sons A/S. Published by Blackwell Publishing Ltd

BCG vaccination and experimental protocol for allergen-induced asthmatic model

The details are presented in Supplement S1.

Analysis of BALF

The details are presented in Supplement S1.

Lymphocyte isolation from the lung, spleen, and lymph nodes

The details are presented in Supplement S1.

Preparation of lung homogenate

The details are presented in Supplement S1.

Histological analysis of the lungs

The details are presented in Supplement S1.

Real-time PCR

The details are presented in Supplement S1.

Cell culture, activation, and proliferation assays

The details are presented in Supplement S1.

Analysis of cytokines

The details are presented in Supplement S1.

Flow cytometric analysis

The details are presented in Supplement S1.

$CD4^+$ T-cell isolation

The details are presented in Supplement S1.

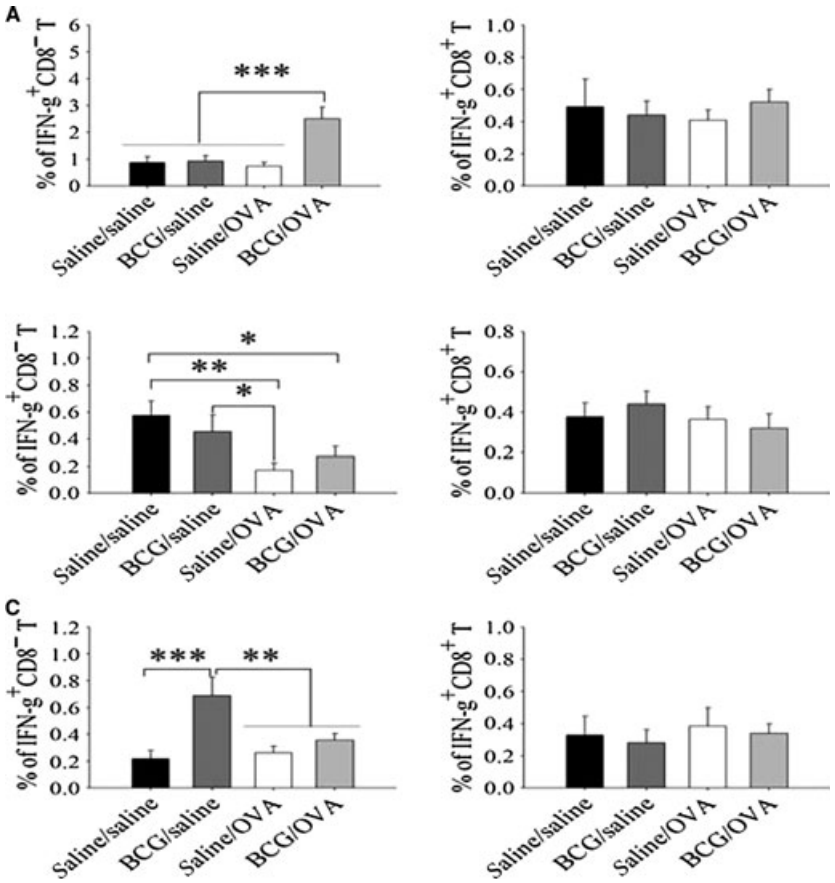

Figure 2 IFN-γ-expressing T cells in different organs. Newborn mice were injected with saline or BCG and sensitized/challenged with saline or OVA later (termed saline/saline, saline/OVA, BCG/saline, and BCG/OVA). Forty-eight hours after the last OVA challenge, their spleen, MLN, and ILN were dissected out for further analysis. Lymphocytes were prepared and stimulated with PMA/ionomycin for 5 h. The cells were then stained with PE-Cy5-CD3, FITC-CD8, and PE-IFN-γ and gated on CD3 for FACS analysis. (A–C) IFN-γ-expressing $CD3^+CD8^-$ ($CD4^+$ T cells) and $CD3^+CD8^+$ T cells in the spleen (A), MLN (B), and ILN (C). Data are expressed as the mean ± SEM of individual groups ($n = 6$–8 mice per group) from two separate experiments, $^*P < 0.05$; $^{**}P < 0.01$; $^{***}P < 0.001$.

© 2013 John Wiley & Sons A/S. Published by Blackwell Publishing Ltd

Adoptive transfer assay

Neonatal C57BL/6 mice were vaccinated with BCG or injected with saline. These mice at 12 weeks of age were killed and their $CD4^+$ T cells from the ILN or spleen were isolated as donor cells, respectively. The purified $CD4^+$ T cells from the ILN or spleen were transferred intravenously into individual C57BL/6 recipients (2×10^6/mouse) that had been sensitized *i.p.* with OVA/alum; 24 h later, the recipients were challenged with 1.0% OVA for three consecutive days. After the last OVA challenge, airway inflammation of individual mice was measured. To characterize the migration of $CD4^+$ T cells *in vivo*, the purified $CD4^+$ T cells from the ILN of BCG-vaccinated or control mice were labeled with 0.2-μm 5-(and-6)-carboxyfluorescein diacetate, succinimidyl ester (CFSE) for 5 mins *in vitro* and washed; the CFSE-labeled $CD4^+$ T cells (2×10^6/mouse) were used for the adoptive transfer assay, as described above. Forty-eight hours after the last OVA challenge, the frequency of ILN $CD4^+$ T cells in the lungs was analyzed by flow cytometry.

ILN resection

Neonatal C57BL/6 mice were vaccinated with BCG or injected with saline. The ILN from the mice was excised surgically 10 days before OVA challenge (termed BCG/ILN excision/OVA and saline/ILN excision/OVA), and the ILN from the mice without BCG vaccination and OVA challenge was also excised as the control (termed saline/ILN excision/saline). The wound was usually healed within 7 days after the operation.

Chemotaxis assay

The details are presented in Supplement S1.

Statistical analysis

Data are expressed as the mean ± SEM. Data were analyzed for their normality by the Kolmogorov–Smirnov test. Differences in normally distributed data among the groups were analyzed by one-way analysis of variance (one-way ANOVA) or by an unpaired Student's *t*-test using SPSS 13.0 software. The Kruskal–Wallis H-test was used for non-normal data. A P value of ≤ 0.05 was considered statistically significant.

Results

Neonatal BCG vaccination enhances Th1 cells, but not Th17 or $Foxp3^+CD4^+$ Treg recruitment in the lung after OVA challenge

Similar to our previous study (13), neonatal vaccination with BCG inhibited airway inflammation and mucus production (Fig. S1). Next, the impact of BCG vaccination on the infiltration of T cells in the lung following OVA challenge was examined. Mice were injected with saline or BCG and sensitized/challenged with saline or OVA (termed saline/saline, BCG/saline, saline/OVA, and BCG/OVA). The frequency of IFN-γ^+CD4^+, but not IFN-γ^+CD8^+, IL-$17A^+$, and $Foxp3^+CD4^+$, T cells in the lung of BCG/OVA mice was significantly higher than that in the BCG/saline and saline/saline mice (6.15 ± 0.42% *vs* 1.47 ± 0.14% and 6.15 ± 0.42% *vs* 1.24 ± 0.07%, respectively, both $P < 0.001$) (Fig. 1).

OVA challenge promotes the migration of BCG vaccination–induced Th1 cells in the ILN

We next sought to examine the origin of the increased Th1 cells in the lung of BCG/OVA mice. The frequency of splenic IFN-γ^+CD4^+, but not IFN-γ^+CD8^+, T cells in the BCG/OVA mice was almost 3-fold higher than that in other groups of mice (all $P < 0.001$) (Fig. 2A), but MLN IFN-γ^+CD4^+ T cells in the OVA-challenged mice was significantly lower than that in the nonchallenged mice (Fig. 2B). These findings suggest that OVA challenge–induced Th2 responses in MLN counteracted the development of Th1 cells (21, 22). The percentage of ILN IFN-γ^+CD4^+, but not IFN-γ^+CD8^+, T cells in the ILN of BCG/saline mice was

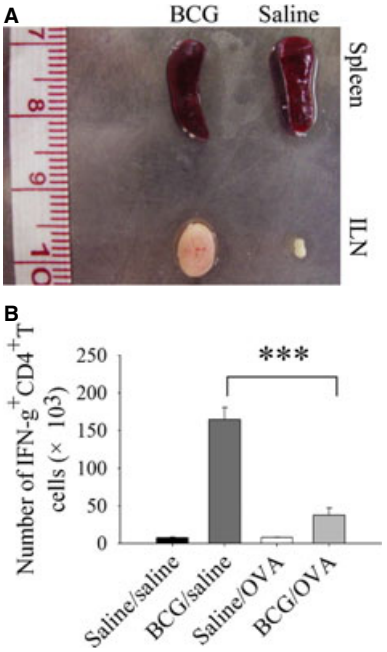

Figure 3 The size of ILN and the number of IFN-γ-expressing $CD4^+$ T cells in the ILN of BCG-vaccinated mice. Newborn mice were injected with saline or BCG and sensitized/challenged with saline or OVA later (termed saline/saline, saline/OVA, BCG/saline, and BCG/OVA). Forty-eight hours after the last OVA challenge, their spleens and ILN were dissected out for further analysis. (A) Morphologies of the ILN and spleen. (B) The number of IFN-γ-expressing $CD4^+$ T cells in the ILN. Lymphocytes were prepared and stimulated with PMA/ionomycin for 5 h. The cells were then stained with PE-Cy5-CD3, FITC-CD8, and PE-IFN-γ and gated on CD3 for FACS analysis. $CD3^+CD8^-$ T cells were considered as $CD4^+$ T cells in this experiment. The number of IFN-γ^+CD4^+ T cells in the ILN = the frequency of IFN-γ^+CD4^+ T cells in the ILN× total cell counts in the ILN. Data are expressed as the mean ± SEM of individual groups (n = 6–8 mice per group) from two separate experiments, ***$P < 0.001$.

© 2013 John Wiley & Sons A/S. Published by Blackwell Publishing Ltd

significantly higher than that in BCG/OVA mice ($0.69 \pm 0.14\%$ *vs* $0.36 \pm 0.05\%$, $P < 0.01$) (Fig. 2C). The ILN size, but not the spleen, from the BCG-vaccinated mice was significantly larger than that from the saline mice (Fig. 3A), accompanied with significantly increased total numbers of ILN lymphocytes (data not shown). Of note, the number of IFN-γ-expressing $CD4^+$ T cells in the BCG-vaccinated ILN was reduced by 77.15% after OVA challenge ($164.61 \pm 16.21 \times 10^3$ *vs* $37.61 \pm 9.52 \times 10^3$, $P < 0.001$) (Fig. 3B). These results suggested that OVA challenge triggered a migration of Th1 cells out of the ILN.

Phenotype and function of $CD4^+$ T cells in the ILN of BCG-vaccinated mice

$CD4^+$ T cells can be divided into naive ($CD44^{low}CD62^{high}$ Tnaive), central memory ($CD44^{high}CD62^{high}$ Tcm), and effector/memory T cells ($CD44^{high}CD62L^{low}$ Tef/em) (23–25). In

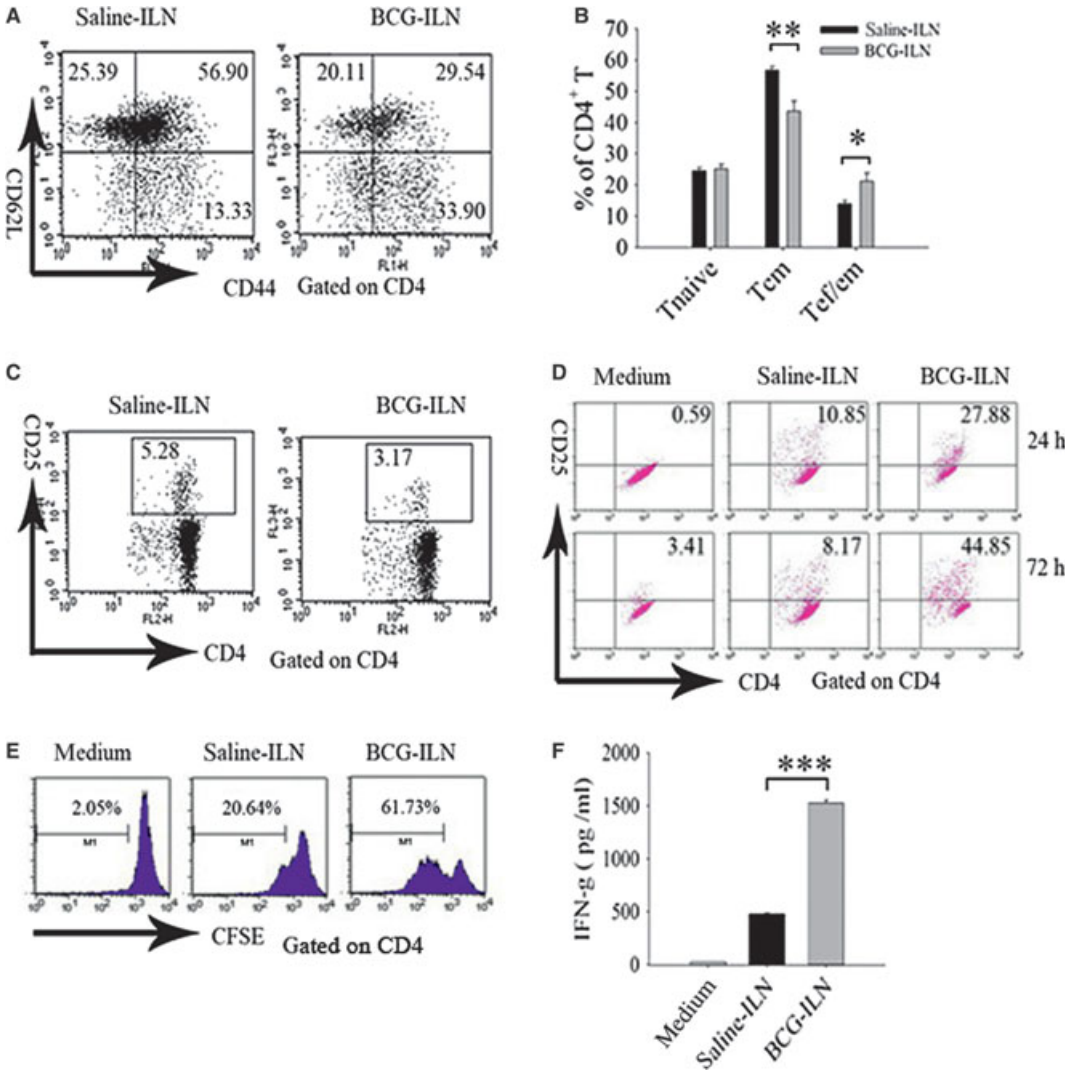

Figure 4 Phenotype and functional analysis of $CD4^+$ T cells in the ILN. Neonatal mice were vaccinated with saline or BCG. At 12 weeks of age, their ILNs were dissected and their lymphocytes were isolated for further analysis. (A and B) Representative FCM plots (A) and quantitative analysis (B) of naive $CD4^+$ T cells ($CD44^{low}CD62L^{high}$, Tnaive), effector/effector memory $CD4^+$ T cells ($CD44^{high}CD62L^{low}$, Tef/em) and central memory $CD4^+$ T cells ($CD44^{high}CD62L^{high}$) in the ILN. Lymphocytes from the ILNs were stained with antibodies against CD4, CD62L, and CD44 and gated on CD4 for FACS analysis. Data are shown as the mean ± SEM ($n = 3$–5 mice per group, $^*P < 0.05$; $^{**}P < 0.01$). (C and D) FCM plots of $CD25^+CD4^+$ T cells in the ILN without *in vitro* stimulation (C) or stimulated with anti-CD3ε/CD28 *in vitro* for the indicated periods (D). (E) The proliferation of $CD4^+$ T cells in the ILN was determined by CFSE dilution assay. These results in (C), (D), and (E) present one of the two independent experiments with similar results ($n = 3$–5 per group for each experiment). (F) The concentrations of IFN-γ in the supernatants of cultured lymphocytes from the ILN were detected by ELISA. Data are shown as the mean ± SEM of individual groups ($n = 3$–5 mice per group) from two separate experiments; $^{***}P < 0.001$.

© 2013 John Wiley & Sons A/S. Published by Blackwell Publishing Ltd

comparison with the other groups, increased frequency of ILN Tef/em, but decreased Tcm cells were detected in the BCG-vaccinated mice (Fig. 4A and 4B). Following anti-CD3e/CD28 stimulation, significantly higher frequency of ILN $CD25^+CD4^+$ T cells was observed in the BCG-vaccinated mice (Fig. 4C and D). The CFSE-labeled ILN $CD4^+$ T cells from the BCG-vaccinated mice displayed more divisions than controls (Fig. 4E), accompanied by significantly higher level of IFN-γ production (1526.36 ± 27.13 *vs* 477.96 ± 6.73 pg/ml, $P < 0.001$) (Fig. 4F). Therefore, these BCG vaccination–induced $CD4^+$ T cells in the ILN exhibited high potentials of activation, proliferation, and IFN-γ secretion *in vitro*.

Distant ILN Th1 cells have potential to migrate into inflamed lungs and directly inhibit airway inflammation

To test the function, ILN or splenic $CD4^+$ T cells from the BCG-vaccinated or saline-injected mice or control PBS were transfused into OVA-sensitized mice (termed BCG-ILN/OVA, saline-ILN/OVA, BCG-spleen/OVA, saline-spleen/OVA, or PBS/OVA). The BCG-ILN/OVA mice displayed less eosinophil infiltrates, pulmonary inflammation, and mucus production, but higher IFN-γ in BALF and greater number of $CFSE^+CD4^+$ T cells in the lung than the other groups (Fig. 5). However, adoptive transfer with the same number of splenic $CD4^+$ T cells failed to modulate airway inflammation and mucus production (data not shown). As expected, the protection of ILN $CD4^+$ T cells was abrogated by pre-surgical removal of the ILN from the BCG-vaccinated mice following OVA challenge (Fig. S2), indicating the importance of ILN $CD4^+$ T cells.

High levels of CXCR3 expression on $CD4^+$ T cells in the ILN from the BCG-vaccinated mice and high levels of CXCL9 expression in the OVA-challenged lungs are associated with the potential of $CD4^+$ T-cell migration

The relative levels of CXCR3, but not CCR5 and CXCR6, mRNA transcripts in the ILN of BCG-vaccinated mice were 3-fold higher than those in the control mice (Fig. 6A). The relative levels of CXCL9, CXCL10, and CXCL11 mRNA transcripts in the lung from the OVA-challenged mice were

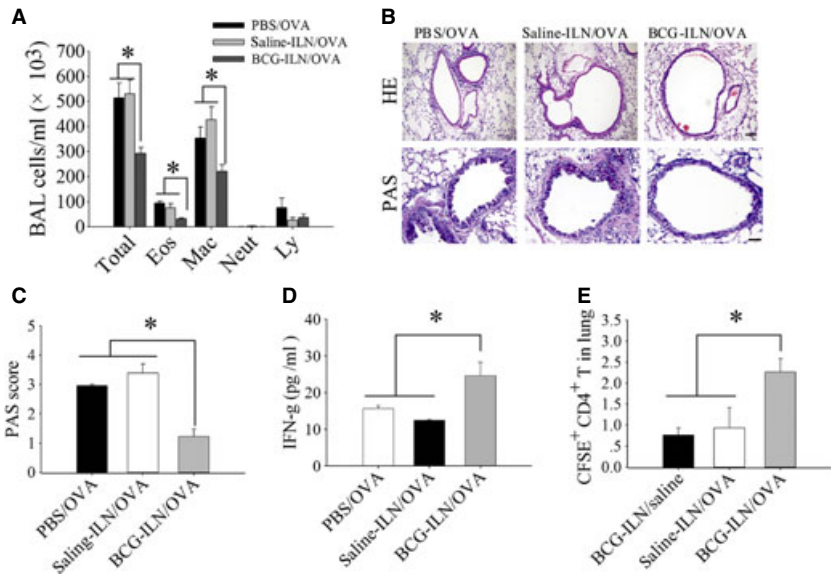

Figure 5 Adoptive transfer of $CD4^+$ T cells from the ILN of BCG-vaccinated mice attenuates allergic airway inflammation. (A–D) $CD4^+$ T cells were isolated from the ILNs of the BCG-vaccinated or saline-injected control mice at 12 weeks of age and intravenously transferred into the recipient mice (2×10^6/mouse) that had been sensitized with OVA. One day later, the recipients were challenged with OVA for three consecutive days. Forty-eight hours after the last OVA challenge, the recipients were killed. (A) The numbers of total and differentiated cell counts in BALF. Eos: eosinophils, Mac: macrophages, Neut: neutrophils, and Ly: lymphocytes. Data are expressed as the mean ± SEM of individual groups (n = 8–10 mice per group). $^*P < 0.05$; $^{**}P < 0.01$. (B) Representative photomicrographs of lung inflammation (H&E staining, upper panels) and mucus secretion (PAS staining, lower panels). (Bar = 100 μm). (C) Quantification of mucus production. PAS score was described in Supplement S1. (n = 8–10 mice per group). $^*P < 0.05$. (D) The concentrations of IFN-γ in BALF were detected by ELISA. Data are expressed as the mean ± SEM of individual groups (n = 8–10 mice per group). $^*P < 0.05$. (E) Quantitative analysis of $CFSE^+CD4^+$ T cells in the lung. $CD4^+$ T cells were purified from the ILN of BCG-vaccinated or control mice and labeled with 0.2-μm CFSE. After CFSE labeling, these $CD4^+$ T cells (2×10^6/mouse) were used for the adoptive transfer assay, as described above. The number of $CFSE^+CD4^+$ T cells in the lung = the frequency of $CFSE^+CD4^+$ T cells in the lung × total cell counts in the lung. The control group was considered as the basal level (designated 1), and the other groups were expressed as fold changes compared with that in the control. The fold change values are shown as the mean ± SEM of individual groups (n = 8–10 mice for per group), $^*P < 0.05$.

© 2013 John Wiley & Sons A/S. Published by Blackwell Publishing Ltd

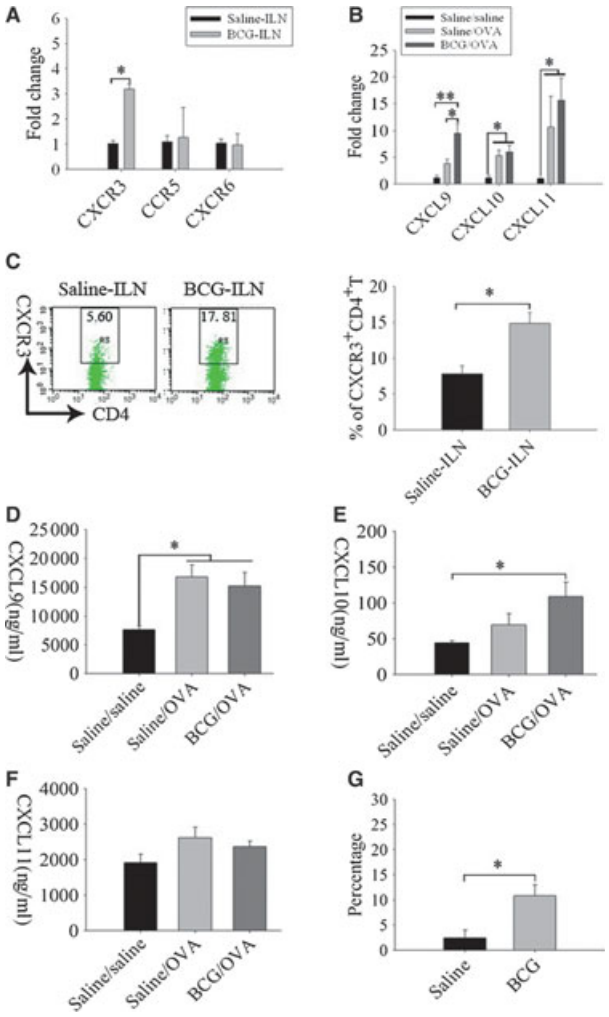

Figure 6 High levels of CXCL9 in the lung of asthmatic mice facilitate the migration of $CD4^+$ T cells from the ILN of BCG-vaccinated mice via high expression of CXCR3. (A and B) The relative levels of CXCR3, CCR5, and CXCR6 mRNA transcripts in the ILN (A) and CXCL9, CXCL10, and CXCL11 in the lung (B) were determined by real-time PCR. Data are expressed as the mean ± SEM of individual groups of mice from two independent experiments. (n = 6–8 mice per group, *P<0.05; **P<0.01). (C) Representative FCM plots (left panels) and the quantified analysis (right panels) of $CXCR3^+CD4^+$ T cells in the ILN from mice vaccinated with or without BCG. The cells were gated on CD4 for FACS analysis. Data are expressed as the mean ± SEM of individual groups (n = 3–4 mice per group) from two independent experiments, *$P < 0.05$. (D–F) The concentrations of CXCL9 (D), CXCL10 (E), and CXCL11 (F) in the lung homogenates were tested by ELISA. Data are expressed as the mean ± SEM of individual groups of mice (n = 6–8 mice per group, *$P < 0.05$). (G) The migration of $CD4^+$ T cells in the ILN of BCG-vaccinated and saline-injected mice in response to chemokine CXCL9 *in vitro*. $CD4^+$ T cells were isolated and their chemotactic responses to CXCL9 were analyzed by transwell assay as described in Supplement S1. Data are expressed as the mean% ± SEM of individual groups of mice from two independent experiments. (n = 4–6 mice per group, *$P < 0.05$).

significantly higher than those in the control mice (Fig. 6B). In addition, BCG vaccination increased the CXCR3 protein expression on $CD4^+$ T cells in the ILN compared with that in the controls ($14.84 \pm 1.49\%$ *vs* $7.84 \pm 1.12\%$, $P < 0.05$) (Fig. 6C). The concentrations of CXCL9 and CXCL10, but not CXCL11, in the lung of BCG/OVA mice were significantly higher than those in the saline/saline mice (Fig. 6D). Furthermore, dramatically increased frequency of migrated ILN $CD4^+$ T cells, in response to CXCL9, was detected in the BCG-vaccinated mice ($10.83 \pm 2.15\%$ *vs* $2.42 \pm 1.59\%$, $P < 0.05$) (Fig. 6G).

Discussion

In this study, the ILN was identified as a pool of Th1 cells and contributed to the protective effects of neonatal BCG vaccination on allergen-induced airway inflammation. Our data have several implications for understanding the mechanisms of BCG vaccination for the prevention of allergic airway inflammation. First, we have confirmed that enhanced Th1 immune responses induced by neonatal BCG vaccination play a central role. Importantly, we have demonstrated, for the first time, that it is the distant draining lymph nodes, ILN, but not the spleen or MLN, that serve as the source of Th1 cells induced by BCG vaccination. Upon OVA challenge, the increased Th1 cells migrate from the ILN into the inflamed lung. Meanwhile, we have examined the possible role of CXCR3 and its chemoattractant, CXCL9, in the regulation of Th1-cell migration.

Previous studies have suggested that the IFN-γ^+ T cells in the inflamed lung come from the migration of circulating T cells and/or the rapid expansion of residual memory $CD4^+$ and $CD8^+$ T cells in the lung after BCG vaccination or *M. tb* chronic infection (18, 26, 27). However, adoptive transfer of effector/memory T cells from the lung shows no evidence of substantial and rapid expansion and beneficial effect in Rag-/- mice (18, 26). It is possible that these cells are not long-lived memory T cells and cannot generate a rapid recall response to secondary pathogen challenge (28). Indeed, live BCG, following *s.c.* vaccination, cannot reach distant lung tissue (26), making it impossible to establish effector T cells in the lung. Furthermore, treatment with antibiotics usually does not effectively remove all mycobacterial antigens (26, 29, 30), and the continual presence of mycobacterial antigens makes difficult to generate mycobacteria-specific memory T-cell immunity (17, 18). We found a higher frequency of IFN-γ^+CD4^+ T cells in the ILN of BCG-vaccinated mice under the steady-state condition, which was significantly reduced following OVA challenge in mice, accompanied by increased number of IFN-γ^+CD4^+ T cells in the inflamed lung. Furthermore, these IFN-γ^+CD4^+ T cells displayed Tef/em phenotype and have potentials to activate, proliferate, and secrete IFN-γ following stimulation *in vitro*. These data suggest that the stored Th1 cells already migrated from the ILN to the lung. Indeed, surgical removal of the ILN prior to OVA challenge almost completed abrogated an increase in the number of IFN-γ^+CD4^+ T cells in the inflamed lung of mice. These data indicate that the ILN serves as a pool of BCG-induced Th1 cells.

© 2013 John Wiley & Sons A/S. Published by Blackwell Publishing Ltd

Adoptive transfer experiments show that $CD4^+$ T cells from the ILN of BCG-vaccinated mice inhibit the increase in allergic airway inflammation and mucus production. The protective effects of adoptive transfer $CD4^+$ T cells from the ILN of BCG-vaccinated mice are associated with an increase in the levels of IFN-γ in BALF (Fig. 5C), which suggests the possibility that more IFN-γ-producing T cells move into the inflamed lung. To address this issue, we labeled $CD4^+$ T cells with CFSE and found that more $CD4^+$ T cells from the BCG-vaccinated ILN move into the inflamed lung tissue. Similar to our results, Fonseca et al. (31) have also found that BCG antigen–induced Th1 cells migrate into the OVA-challenged lung and secrete IFN-γ to counteract the OVA-induced Th2 response and subsequent allergic airway inflammation. These studies suggest that the accumulation of IFN-γ-producing $CD4^+$ T cells in the lung by *s.c.* BCG vaccination plays a critical protective role in the subsequent development of asthma. To further confirm the idea that the importance of increased IFN-γ-expressing T cells in the ILN against allergic airway inflammation, we performed a surgical excision of the ILN before OVA challenge to completely deplete the effect of IFN-γ-expressing T cells in the ILN. As expected, the protective effects of BCG vaccination on allergic airway inflammation are lost following the ILN excision, and the loss of this protection is associated with a decrease in the frequency of IFN-γ-expressing $CD4^+$, but not $CD8^+$, T cells in the inflamed lung.

Chemokines and their corresponding receptors are crucial for the migration of $CD4^+$ T cells into inflamed tissue. Thus, we measured Th1-associated chemokines in the OVA-challenged lung. After OVA challenge, the levels of CXCL9, a ligand for CXCR3, expression in the lung were significantly up-regulated in the current study regardless of BCG vaccination; however, increased frequency of Th1 cells only occurred in the lung of BCG/OVA mice. This is partially explained by the fact that BCG vaccination promoted the expression of CXCR3 on $CD4^+$ T cells in the ILN. This result supports the idea that CXCR3 expression level is a principal factor determining both the ability to respond and the intensity of response to CXCR3 ligands in environmental antigen responses (32). Transwell migration assays further demonstrate that $CD4^+$ T cells from the ILN of BCG-vaccinated mice can potentially migrate in response to CXCL9. Therefore, these results suggest that high levels of CXCR3 expression on $CD4^+$ T cells in the ILN of BCG-vaccinated mice and high concentrations of CXCL9, the Th1-associated chemokine, in the lungs may be the basis for the migration of Th1 cells from the ILN of BCG-vaccinated mice into the inflamed lung upon OVA challenge. However, further *in vivo* experiments are needed to determine the exact role of CXCR3 and CXCL9 in the migration of Th1 cells.

In summary, our data indicate the distant draining lymph node (ILN) as a 'weapon' pool of IFN-γ-expressing $CD4^+$ T cells induced by neonatal BCG vaccination. These Th1 cells are resting in steady state and are ready for migrating into the inflamed lung through the CXCR3–CXCL9 axis, subsequently inhibiting allergen-induced airway inflammation.

Acknowledgments

We would like to thank Drs. Ming Yan (College of Biomedical Engineering & Instrument Science, Zhejiang University), Zhijian Cai (Institute of Immunology, Zhejiang University), Yungui Wang (Institute of Hematology, Zhejiang University), and Youfa Zhu (Department of Pathology, Zhejiang University) for their technical assistance. This study was supported in part by the grants from National Natural Science Foundation of China for Distinguished Young Scholars (No. 30825019, Shen HH) and National Natural Science Foundation of China (No. 81070013, Shen HH), and Major and Key Program of Zhejiang Province (2008C03002-2, Li W).

Author contributions

Gen-sheng Zhang and Ping-li Wang contributed to the design of the experiments, acquisition and analysis of the data and also contributed to the initial draft writing of this manuscript. Zhang-wei Qiu, Xue-jun Qin, Xiao-ping Lin, Na Li, Hua-qiong Huang, Hui Liu, and Wen Hua contributed to the collection and analysis and interpretation of data. Wen Li and Zhi-hua Chen contributed to the design and assessment of data and revised the manuscript. Hang Zhao provided a critical review and revision of the manuscript. Hua-hao Shen contributed to conception and design of the experiments, involved in the interpretation of experimental results, revised this manuscript and contributed to final approval of the version to be published.

Conflict of interest

The authors have declared no conflict of interest in the publication of this manuscript.

Supporting Information

Additional Supporting Information may be found in the online version of this article:

Supplement S1. Supplemental materials and methods.

Figure S1. Neonatal BCG vaccination inhibits allergic airway inflammation in C57BL/6 mice.

Figure S2. IFN-γ-producing $CD4^+$ T cells in the ILN from the BCG-vaccinated mice are indispensable for the suppression of airway inflammation of allergic asthma.

Table S1. Primer sequences for real-time PCR.

References

1. Cohn L, Elias JA, Chupp GL. Asthma: mechanisms of disease persistence and progression. *Annu Rev Immunol* 2004;**22**: 789–815.
2. Eapen SS, Busse WW. Asthma. *Clin Allergy Immunol* 2002;**16**:325–353.
3. Umetsu DT, McIntire JJ, Akbari O, Macaubas C, DeKruyff RH. Asthma: an epidemic of dysregulated immunity. *Nat Immunol* 2002;**3**:715–720.
4. Wills-Karp M. Immunologic basis of antigen-induced airway

© 2013 John Wiley & Sons A/S. Published by Blackwell Publishing Ltd

hyperresponsiveness. *Annu Rev Immunol* 1999;**17**:255–281.
5. Gavett SH, O'Hearn DJ, Li X, Huang SK, Finkelman FD, Wills-Karp M. Interleukin 12 inhibits antigen-induced airway hyperresponsiveness, inflammation, and Th2 cytokine expression in mice. *J Exp Med* 1995;**182**:1527–1536.
6. Iwamoto I, Kumano K, Kasai M, Kurasawa K, Nakao A. Interleukin-12 prevents antigen-induced eosinophil recruitment into mouse airways. *Am J Respir Crit Care Med* 1996;**154**:1257–1260.
7. Herz U, Gerhold K, Gruber C, Braun A, Wahn U, Renz H et al. BCG infection suppresses allergic sensitization and development of increased airway reactivity in an animal model. *J Allergy Clin Immunol* 1998;**102**:867–874.
8. Hopfenspirger MT, Agrawal DK. Airway hyperresponsiveness, late allergic response, and eosinophilia are reversed with mycobacterial antigens in ovalbumin-presensitized mice. *J Immunol* 2002;**168**:2516–2522.
9. Hubeau C, Singer M, Lagranderie M, Marchal G, Vargaftig B. Extended freeze-dried Mycobacterium bovis Bacillus Calmette-Guerin induces the release of interleukin-12 but not tumour necrosis factor-alpha by alveolar macrophages, both *in vitro* and *in vivo*. *Clin Exp Allergy* 2003;**33**:386–393.
10. Lagranderie M, Nahori MA, Balazuc AM, Kiefer-Biasizzo H, Lapa e Silva JR, Milon G et al. Dendritic cells recruited to the lung shortly after intranasal delivery of Mycobacterium bovis BCG drive the primary immune response towards a type 1 cytokine production. *Immunology* 2003;**108**:352–364.
11. Oliveira FH, Sarinho SW, Montenegro S, Neuenschwander C, Queiroz R, Medeiros D et al. Production of interferon gamma in asthmatic patients with small bacille Calmette-Guerin scars: a pilot study. *Allergy Asthma Proc* 2006;**27**:516–522.
12. Vargas MH, Bernal-Alcantara DA, Vaca MA, Franco-Marina F, Lascurain R. Effect of BCG vaccination in asthmatic schoolchildren. *Pediatr Allergy Immunol* 2004;**15**:415–420.
13. Shen H, Huang H, Wang J, Ye S, Li W, Wang K et al. Neonatal vaccination with Bacillus Calmette-Guerin elicits long-term protection in mouse-allergic responses. *Allergy* 2008;**63**:555–563.
14. Christ AP, Rodriguez D, Bortolatto J, Borducchi E, Keller A, Mucida D et al. Enhancement of Th1 lung immunity induced by recombinant Mycobacterium bovis Bacillus Calmette-Guerin attenuates airway allergic disease. *Am J Respir Cell Mol Biol* 2010;**43**:243–252.
15. Jung YJ, Ryan L, LaCourse R, North RJ. Properties and protective value of the secondary versus primary T helper type 1 response to airborne Mycobacterium tuberculosis infection in mice. *J Exp Med* 2005;**201**:1915–1924.
16. Khader SA, Bell GK, Pearl JE, Fountain JJ, Rangel-Moreno J, Cilley GE et al. IL-23 and IL-17 in the establishment of protective pulmonary CD4 + T cell responses after vaccination and during Mycobacterium tuberculosis challenge. *Nat Immunol* 2007;**8**:369–377.
17. Bevan MJ. Immunology: remembrance of things past. *Nature* 2002;**420**:748–749.
18. Kipnis A, Irwin S, Izzo AA, Basaraba RJ, Orme IM. Memory T lymphocytes generated by Mycobacterium bovis BCG vaccination reside within a CD4 CD44lo CD62 Ligandhi population. *Infect Immun* 2005;**73**:7759–7764.
19. Mora JR, von Andrian UH. T-cell homing specificity and plasticity: new concepts and future challenges. *Trends Immunol* 2006;**27**:235–243.
20. Westermann J, Ehlers EM, Exton MS, Kaiser M, Bode U. Migration of naive, effector and memory T cells: implications for the regulation of immune responses. *Immunol Rev* 2001;**184**:20–37.
21. Cai Y, Zhou J, Webb DC. Treatment of mice with fenbendazole attenuates allergic airways inflammation and Th2 cytokine production in a model of asthma. *Immunol Cell Biol* 2009;**87**:623–629.
22. Idzko M, Hammad H, van Nimwegen M, Kool M, Muller T, Soullie T et al. Local application of FTY720 to the lung abrogates experimental asthma by altering dendritic cell function. *J Clin Invest* 2006;**116**:2935–2944.
23. Martin-Fontecha A, Baumjohann D, Guarda G, Reboldi A, Hons M, Lanzavecchia A et al. CD40L+ CD4 + memory T cells migrate in a CD62P-dependent fashion into reactive lymph nodes and license dendritic cells for T cell priming. *J Exp Med* 2008;**205**:2561–2574.
24. Pakpour N, Zaph C, Scott P. The central memory CD4 + T cell population generated during Leishmania major infection requires IL-12 to produce IFN-gamma. *J Immunol* 2008;**180**:8299–8305.
25. Yuan X, Paez-Cortez J, Schmitt-Knosalla I, D'Addio F, Mfarrej B, Donnarumma M et al. A novel role of CD4 Th17 cells in mediating cardiac allograft rejection and vasculopathy. *J Exp Med* 2008;**205**:3133–3144.
26. Henao-Tamayo MI, Ordway DJ, Irwin SM, Shang S, Shanley C, Orme IM. Phenotypic definition of effector and memory T-lymphocyte subsets in mice chronically infected with Mycobacterium tuberculosis. *Clin Vaccine Immunol* 2010;**17**:618–625.
27. Connor LM, Harvie MC, Rich FJ, Quinn KM, Brinkmann V, Le Gros G et al. A key role for lung-resident memory lymphocytes in protective immune responses after BCG vaccination. *Eur J Immunol* 2010;**40**:2482–2492.
28. Badovinac VP, Porter BB, Harty JT. Programmed contraction of CD8(+) T cells after infection. *Nat Immunol* 2002;**3**:619–626.
29. Mathurin KS, Martens GW, Kornfeld H, Welsh RM. CD4 T-cell-mediated heterologous immunity between mycobacteria and poxviruses. *J Virol* 2009;**83**:3528–3539.
30. Orme IM, Andersen P, Boom WH. T cell response to Mycobacterium tuberculosis. *J Infect Dis* 1993;**167**:1481–1497.
31. Fonseca DM, Paula MO, Wowk PF, Campos LW, Gembre AF, Turato WM et al. IFN-gamma-mediated efficacy of allergen-free immunotherapy using mycobacterial antigens and CpG-ODN. *Immunol Cell Biol* 2011;**89**:777–785.
32. Campbell JD, Gangur V, Simons FE, Hay-Glass KT. Allergic humans are hyporesponsive to a CXCR3 ligand-mediated Th1 immunity-promoting loop. *FASEB J* 2004;**18**:329–331.

© 2013 John Wiley & Sons A/S. Published by Blackwell Publishing Ltd

Supplemental Information

Distant lymph nodes serve as pools of Th1 cells induced by neonatal BCG vaccination for the prevention of asthma in mice

Name and full postal address of the corresponding author

Hua-Hao Shen,

Department of Respiratory and Critical Care Medicine, Second Affiliated Hospital, Zhejiang University School of Medicine, Hangzhou 310009, P.R.China.

Phone: (86) 571 87783729;

Fax: (86) 571 87783729;

Email: hh_shen@yahoo.com.cn

Supplemental Materials and Methods

BCG vaccination and experimental protocol for allergen-induced asthmatic model

Freeze-dried living BCG (D2-BP302 strain, Biological Institute of Shanghai, China) was applied in the current study, as described previously (1). In brief, individual mice at birth (day 0) were injected subcutaneously (*s.c.*) with 25 μl BCG suspension [10^5 infection units (IU)] in saline at the base of tail, where the draining lymph nodes are ILN. Mice were boosted twice with the same dose on days 7 and 14. Control mice were injected with the same amount of saline**.**

Allergen-induced asthma model was established, as described previously (13). In brief, individual mice were sensitized by intraperitoneally (*i.p.*) injecting with 20 μg chicken OVA (Sigma-Aldrich, St Louis, MO, USA) emulsified in 100 μl Imject Alum (Pierce, Rockford, IL, USA) or saline (control) on days 56 and 70. Subsequently, the mice were challenged with aerosolized OVA (1% in saline for 40 min) or saline (control) three times between days 80 and 82.

Analysis of BALF

Collection of BALF was performed 48 hours (h) after the last OVA challenge. Inflammatory cells were obtained by cannulation of the trachea and lavage of the airway lumen with 0.8 ml PBS. Cytospin slides were prepared for Wright-Giemsa staining. The numbers of total and different types of inflammatory cells were counted in a blind fashion.

Lymphocyte isolation from the lung, spleen and lymph nodes

The lungs were perfused, cut into small pieces, and digested with collagenase type I (1 mg/ml, Sigma-Aldrich) and 150 μg/ml of DNase I (Sigma-Aldrich) at 37° C for 1 h,

followed by crushing the pieces of tissue through a 40 μm cell strainer. The splenic and lymph node single-cell suspensions were obtained by gently mincing these tissues using the plunger of a 5 ml syringe followed by passing through a 40-μm cell strainer. Lymphocytes were separated with Lympholyte®-M cell separation media (EZ-Sep™ Mouse 1X, Dakewe Bio, China), according to the manufacturer's instruction.

Preparation of lung homogenate

The frozen lung tissue samples were weighed and homogenized in RPMI 1640 medium (100 mg tissue per milliliter) on ice. The homogenates were centrifuged at 3000 × g for 15 minutes. The supernatant was collected for the determination of cytokines.

Histological analysis of the lungs

Paraffin-embedded lung tissue sections (5 μm) were stained with hematoxylin and eosin (H&E) and periodic acid-Schiff (PAS) to evaluate pulmonary inflammatory cell infiltration and mucus production. An arbitrary scoring system was used to quantify the mucus production (2). In brief, the PAS-stained goblet cells and total numbers of epithelial cells in airway epithelium were counted in a blinded manner using a numerical scoring system (0, <5%; 1, 5–25%; 2, 25–50%; 3, 50–75%; and 4, >75% goblet cells). At least 5 bronchioles were counted in each slide from each mouse, and the sum of the airway scores from each lung was divided by the number of airways examined (n=eight to ten mice per group).

Real-time PCR

Total RNA was extracted from different tissues using TRIzol according to the manufacturer's instructions (Invitrogen) and reversely transcribed into cDNA using

random hexamers and superscript II reverse transcriptase (Invitrogen). The relative levels of CXCR3, CXCR6, CCR5, CXCL9, CXCL10 and CXCL11 mRNA transcripts to control -actin were determined by quantitative RT-PCR using the SYBR Green system (Takara, Japan) and specific primers (Online Table S1) on a spectrofluorometric thermal cycler (iCycler; Bio-Rad) and analyzed by $2^{-(\Delta\Delta Ct)}$.

Cell culture, activation and proliferation assays

Lymphocytes from the BCG- or saline-treated ILN at 2×10^5 cells/well were cultured in 1640 medium in 96-well plates at 37 °C in 5% CO_2 and stimulated in triplicate with 5 μg/ml of anti-CD3e and 1 μg/ml of anti-CD28 (eBioscience, San Diego, USA). After culture for 24 and 72 h, these cells were harvested and stained with anti-mouse-CD25 and analyzed by flow cytometry. In another group of experiment, lymphocytes were labeled with 0.2 μM 5-(and-6)-carboxyfluorescein diacetate, succinimidyl ester (CFSE, invitrogen) for 5 mins, and then cultured in 1640 medium at 37 °C in 5% CO_2 and stimulated with the same doses of anti-CD3e and anti-CD28. After culture for 72 h, these cells were harvested for CFSE dilution assays by flow cytometry. The cell culture supernatant was collected and stored at -80 °C for the measurement of cytokines.

Analysis of cytokines

The concentrations of IFN-γ in BALF and culture supernatant were measured using a commercially available ELISA kit (Biosource). The contents of CXCL9, CXCL10 and CXCL11 in the lung homogenates were determined by ELISA using the duoSet® ELISA development kit or quantikine ELISA kit (R&D systems), according to the manufacturer's protocols.

Flow-cytometric analysis

Lymphocytes were stained with PE-, PE-Cy5-, FITC-, or APC-conjugated antibodies against CD4, CD3, CD8, CD25, CD44, CD62L, or CXCR3 (eBioscience). Intracellular staining of Foxp3 was performed with a mouse regulatory T cell staining kit (eBioscience). For intracellular staining of IFN-γ and IL-17A, lymphocytes were stimulated *in vitro* with 10 ng/ml of Phorbol-12-myristate-13-acetate (PMA) and 500 ng/ml of ionomycin for 5 h in the presence of 10 μg/ml of brefeldin A (AleXis), and then stained with antibodies against IFN-γ or IL-17A, respectively. The samples were analyzed using a FACSCalibur flow cytometer and CellQuest software (BD Biosciences). In some experiments, we used the cell phenotype of $CD3^+CD8^-$ T cells to represent $CD4^+$ T cells since the percentage of $CD4^+$ T cells in the total lymphocytes, whether in the spleen or lymph node, was comparable with the proportion of $CD3^+CD8^-$ T cells in our preliminary experiment (data not shown).

$CD4^+$ T cell isolation

$CD4^+$ T cells were purified by negative selection using magnetic beads (Miltenyi Biotec), as described previously (3). The purified $CD4^+$ T cells (with a purity of > 94%) were used for adoptive transfer experiments and chemotaxis assays.

Chemotaxis assay

The purified $CD4^+$ T cells from the ILN were used for chemotaxis assays using 5 μm pore polycarbonate filters in 24-well Transwell chambers (Corning, Costar), as described previously (4). $CD4^+$ T cells at 5×10^5 cells/ml were cultured in 200 μl of 10% fetal calf serum RPMI 1640 in the top chamber while 600 μl of 1% BSA RPMI 1640 alone or

containing 0.5 μg/ml of CXCL9 (R&D Systems) were added into the bottom wells and cultured for 3 h at 37 °C. The $CD4^+$ T cells that had migrated into the bottom wells were counted. The percentage of migrated $CD4^+$ T cells was calculated as follow: Migration (%) = (the number of $CD4^+$ T cells in the bottom chamber with CXCL9—the number of $CD4^+$ T cells in the bottom chamber with medium alone)/the number of $CD4^+$ T cells loaded ×100.

References for supplemental Materials and methods

1. Shen H, Huang H, Wang J, Ye S, Li W, Wang K, et al. Neonatal vaccination with Bacillus Calmette-Guerin elicits long-term protection in mouse-allergic responses. *Allergy* 2008;**63**:555-563.
2. Semitekolou M, Alissafi T, Aggelakopoulou M, Kourepini E, Kariyawasam HH, Kay AB, et al. Activin-A induces regulatory T cells that suppress T helper cell immune responses and protect from allergic airway disease. *J Exp Med* 2009;**206**:1769-1785.
3. Qin XJ, Shi HZ, Deng JM, Liang QL, Jiang J, Ye ZJ. CCL22 recruits CD4-positive CD25-positive regulatory T cells into malignant pleural effusion. *Clin Cancer Res* 2009;**15**:2231-2237.
4. Ben S, Li X, Xu F, Xu W, Li W, Wu Z, et al. Treatment with anti-CC chemokine receptor 3 monoclonal antibody or dexamethasone inhibits the migration and differentiation of bone marrow CD34 progenitor cells in an allergic mouse model. *Allergy* 2008;**63**:1164-1176.

Supplemental Table 1: Primer sequences for real-time PCR.

Primers	Sequences
CXCR3	Fwd 5'- TGA GCA GCA CGG ACA CCT TC-3', Rev 5'-AAC CCA CTG GAC AGC AGC ATC-3';
CCR5	Fwd 5'-GCA AAG GGA CGG ACA C-3', Rev 5'-GGC AGT CAG GCA CAT C-3';
CXCR6	Fwd 5'- GCC AGG AGA ACA AAC G-3', Rev 5'- AGG GCA GAG TAC AGA CAA-3';
CXCL9	Fwd 5'- CCC AAT TGC AAC AAA ACT GA-3', Rev 5'- TTC CCC CTC TTT TGC TTT TT-3';
CXCL10	Fwd 5'- TGA ATC CGG AAT CTA AGA CCA-3', Rev 5'- GAG GCT CTC TGC TGT CCA TC-3';
CXCL11	Fwd 5'- CAA GCA AGC TCG CCT CAT A-3', Rev 5'- GCA TGT TCC AAG ACA GCA GA-3';
β-actin	Fwd 5'- AGA GGG AAA TCG TGC GTG AC -3', Rev 5'- CAA TAG TGA TGA CCT GGC CGT -3';

Supplemental Figure 1

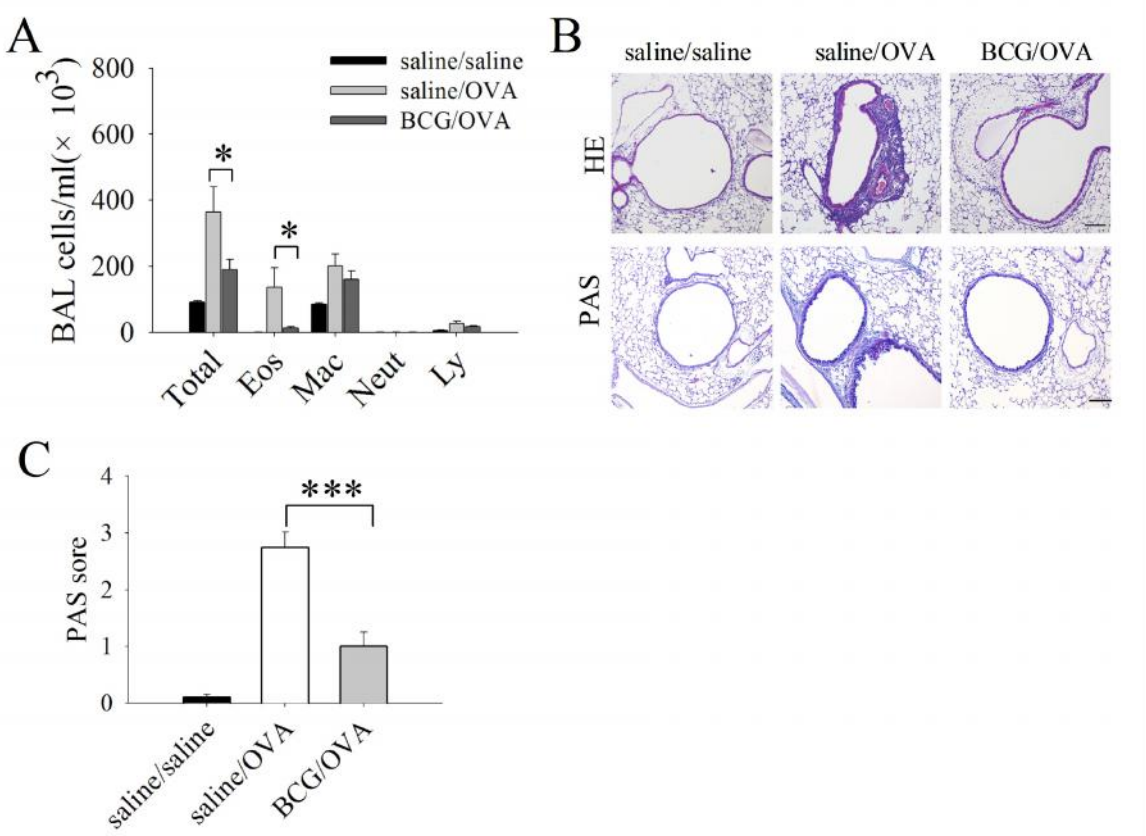

Figure S1: Neonatal BCG vaccination inhibits allergic airway inflammation in C57BL/6 mice**.** Newborn mice were injected with saline or BCG, and sensitized/challenged with OVA later (termed saline/OVA and BCG/OVA). Forty-eight hours after the last OVA challenge, BALF was recovered and lung tissues were dissected. (A) Total and differential cell counts in BALF. Eos: eosinophils, Mac: macrophages, Neut: neutrophils and Ly: lymphcytes. Data are expressed as the mean ± SEM (n=8～10 mice for per group; *****P ＜0.05). (B) Representative photomicrographs of the lung stained with HE (upper panels) or PAS (lower panels). (Bar=100 μm). (C) Quantification of mucus production. PAS score was described in *online supplemental Material and Methods*. (n=8～10 mice per group; *******P ＜0.001).

Supplemental Figure 2

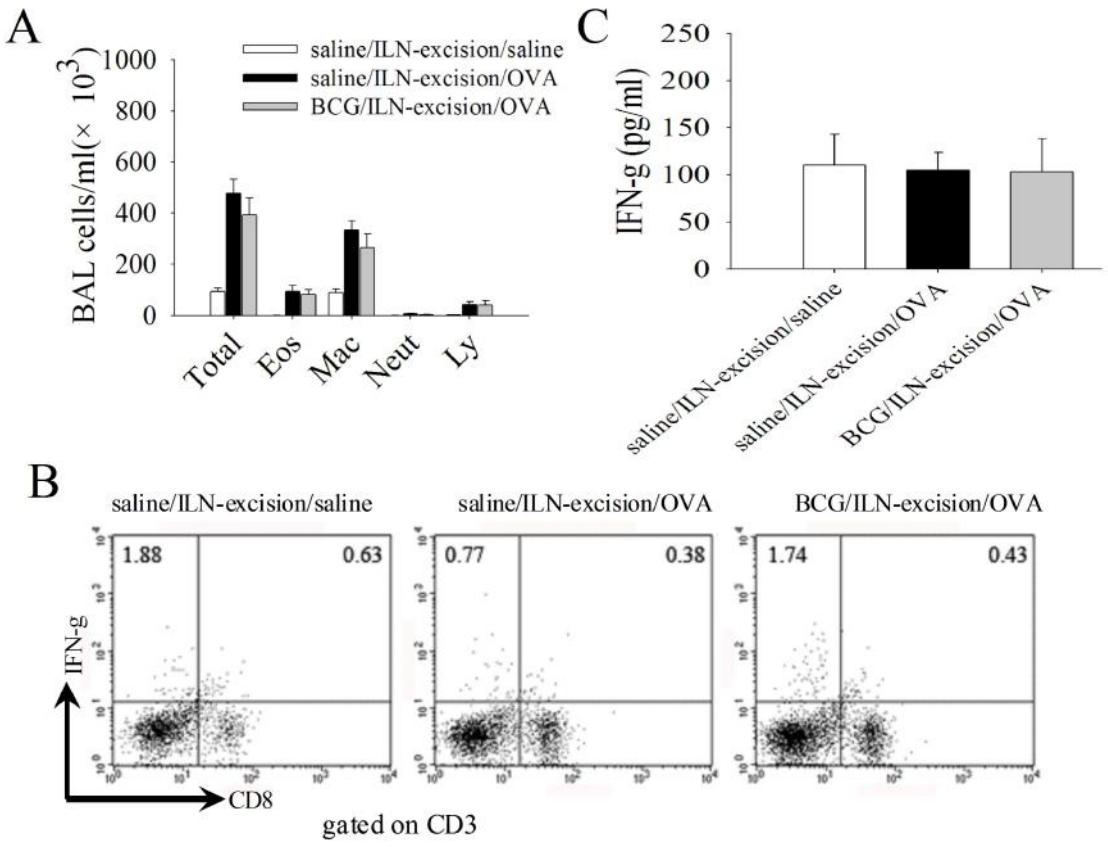

Figure S2: IFN-γ-producing $CD4^+$ T cells in the ILN from the BCG-vaccinated mice are indispensable for the suppression of airway inflammation of allergic asthma. Groups of neonates were vaccinated with BCG or saline and the ILNs of individual mice were excised surgically 10 days prior to OVA challenge (termed BCG/ILN-excision/OVA and saline/ILN-excision/OVA), and a group of mice without BCG vaccination and OVA challenge were also subjected to ILN-excision as the controls (saline/ILN-excision/saline). Forty-eight hours after the last OVA challenge, BALF was recovered and lung tissues were dissected. (A) Total and differentiated cell counts in BALF. Eos: eosinophils, Mac: macrophages, Neut: neutrophils and Ly: lymphcytes. Data are expressed as the mean ± SEM (n=8～10 mice per group). (B) Representative FCM plots

of IFN-γ-expressing $CD3^+CD8^-$ T cells and $CD3^+CD8^+$ T cells in lung in indicated groups. Lung lymphocytes from different groups were prepared and stimulated with PMA/ionomycine *in vitro* for 5 h. The cells were then stained with PE-Cy5-CD3, FITC-CD8 and PE-IFN-γ, and gated on CD3 for FACS analysis. $CD3^+CD8^-$ T cells represent $CD4^+$ T cells in this part experiment. (C) IFN-γ levels in BALF were measured by ELISA. Data are expressed as the mean ± SEM (n=8～10 mice per group).